NASA/TM—2001-211284

Flow Visualization in Evaporating Liquid Drops and Measurement of Dynamic Contact Angles and Spreading Rate

Nengli Zhang
Ohio Aerospace Institute, Brook Park, Ohio

David F. Chao
Glenn Research Center, Cleveland, Ohio

Prepared for the
2001 International Mechanical Engineering Congress and Exposition
sponsored by the American Society of Mechanical Engineers
New York City, New York, November 11–16, 2001

National Aeronautics and
Space Administration

Glenn Research Center

November 2001

Available from

NASA Center for Aerospace Information
7121 Standard Drive
Hanover, MD 21076

National Technical Information Service
5285 Port Royal Road
Springfield, VA 22100

Available electronically at http://gltrs.grc.nasa.gov/GLTRS

FLOW VISUALIZATION IN EVAPORATING LIQUID DROPS AND MEASUREMENT OF DYNAMIC CONTACT ANGLES AND SPREADING RATE

Nengli Zhang* and David F. Chao
National Aeronautics and Space Administration
Glenn Research Center
Cleveland, Ohio 44135

SUMMARY

A new hybrid optical system, consisting of reflection-refracted shadowgraphy and top-view photography, is used to visualize flow phenomena and simultaneously measure the spreading and instant dynamic contact angle in a volatile-liquid drop on a nontransparent substrate. Thermocapillary convection in the drop, induced by evaporation, and the drop real-time profile data are synchronously recorded by video recording systems. Experimental results obtained from this unique technique clearly reveal that thermocapillary convection strongly affects the spreading process and the characteristics of dynamic contact angle of the drop. Comprehensive information of a sessile drop, including the local contact angle along the periphery, the instability of the three-phase contact line, and the deformation of the drop shape is obtained and analyzed.

INTRODUCTION

Most studies on liquid drop spreading have focused on nonvolatile liquid sessile drops for their simplicity both in experimental measurements and theoretical analysis. The occurrence of liquid evaporation is, however, inevitable. The affects of evaporation on the spreading and contact angle become very important for a more complete understanding of these processes. It has been found that evaporation can induce Marangoni-Bénard convection in sessile drops (ref. 1). The fluid flow in the drop is attributable to the surface-tension mechanism from local variations in the surface temperature. The effect of convection in the drop on the wetting and spreading processes, however, is not clear. Flow in a small sessile drop takes place on a microscopic scale and cannot be viewed by eye. Although convective flow, if any, can be observed under a microscope by means of microparticle tracers, the field under investigation is inevitably intruded. Optical methods are the only nonintrusive means of visualizing flow in small fluid volumes. Both the Schlieren method and Mach-Zehnder interferometry, however, are unsuitable for visualizing flow motion in an evaporating sessile drop. The only useful optical method is shadowgraphy (ref. 2).

Shadowgraphy is the simplest of the optical visualizing methods, which is roughly sensitive to changes in the second derivative of the density of the field under investigation (ref. 3). In a locally increasing density field, the fluid acts like a convex lens. In a decreasing density field, it has the effect of a concave lens. When turbulent motion occurs in the field, a fluctuating density creates a distribution of tiny convex and concave lenses that are continuously changing in shape and location. The effect has been utilized to investigate the internal convection in evaporating drops (refs. 2 and 4). A laser-shadowgraphic system developed by Zhang and Yang (ref. 5) was modified and successfully used to visualize the thermocapillary convection inside and to measure the spreading rate of volatile drops, simultaneously (refs. 4 and 6). It was found that evaporation and thermocapillary convection strongly affect the spreading process. Unfortunately, the laser-shadowgraphic system, including its modified version, can only be applied to sessile drops spreading on transparent substrates. Allain et al. (ref. 7) suggested using the reflection of a parallel beam on the surface of a sessile drop to measure the contact angle of the drop on a non-transparent substrate. Obviously, it can work only when the surface of the tested liquid has enough reflectance. However, the light reflectivity on the surface of most common liquids is insufficient and, therefore, this method is rarely applied in practice. Another major disadvantage of this method is that it does not allow visualization of the flow in the drop.

This present paper suggests a hybrid optical system consisting of a reflection-refracted shadowgraphy and top-view photography to simultaneously visualize the convective flow, and measure the dynamic contact angles and spreading rate of volatile sessile drops on a nontransparent substrate.

*Phone: 216–433–8750; Fax: 216–433–8050; e-mail: nzhang@grc.nasa.gov

APPARATUS

Laser reflection-refracted shadowgraphy and direct top-view photography were simultaneously achieved by using a hybrid optical system. The apparatus consisted of a laser light, a white light, a collimator, three beamsplitters, two video recording systems (each consisting by a CCD zoom camera, video recorder and monitor), a test plate (aluminized glass plate), and a screen, as illustrated in figure 1. A uniphase Model 1105p, 10-mW cylindrical helium-neon laser and an Olympus Model Highlight 2000 were used as the laser source and the white-light source, respectively. Both light beams passed through the collimator, Newport Model LC–075, via Beam splitter I, and collimated to parallel beams coincidentally, and then reflected by Beam splitter II to pass perpendicularly through a sessile drop, situated on an aluminized glass plate. The laser beam produced a reflection-refracted image of the sessile drop on a screen, and the white beam provided a sharp photograph of the top view of the drop. The drop top-view was recorded on Video recording system I, and the laser reflection-refracted shadowgraphic image on Video recorder II. The two recorders were controlled synchronously.

Before each test, the aluminized glass plate was cleaned by ethanol and wiped by lens-cleaning tissue, and then shelved in open air, covered by a soft tissue, for at least 24 hr. By this method, the plate surface was freed of residual liquid molecules and remained free of impurities from the ambient air. The test liquid was carefully deposited on the plate by a microsyringe to form a 1.5 to 2.5 μl sessile drop. The origin of spreading and evaporation time was taken as the moment when the microsyringe was detached from the liquid body.

RESULTS AND DISCUSSION

Consider a sessile drop placed in the collimated light beam of the hybrid optical-system so that the hybrid light beam traverses the drop volume from top to bottom and then is reflected out of the volume as shown in figure 1. The detailed path of the beam traveling through the drop is that the collimated incident light is refracted by the sessile drop and then reflected on the substrate surface, returning to the air-liquid interface, and finally refracted out of the drop. The refracted light-beam is directed to the horizontal by Beam splitter III and intercepted by a vertical screen, forming a shadowgraphic image. This is referred to as reflection-refracted shadowgraphic image. As is well known, a small sessile drop can be considered a spherical cap. Consequently, the incident angle of the parallel beam on the drop surface reaches its maximum at the edge of the drop. It is the refracted ray out of the drop edge that forms the outer fringe of the reflection-refracted shadowgraphic image. The detailed optical path at the drop edge is shown in figure 2. The image brightness at a given point is linearly related to the integral average of the second derivative of the refractive index over the passage of a ray, which approximately equals the double of the local height of the drop. The entire image, being a map of the distribution of the average of the second derivative of the refractive index over the ray passage, represents the distribution of the average second derivative of the temperature along the ray passage in the evaporating drop. From a real-time change of the image, the fluid motion in the drop, if any, can be clearly observed.

Figures 3(a) and (b) show an instant top-view photograph and corresponding reflection-refracted shadowgraph of a 2.5 μl silicone-oil (50 cSt) drop, spreading on an aluminized glass plate in open air. The bright circle at the center of the top-view photograph, figure 3(a), is formed by reflection of the parallel light beams at the drop summit. The bright annulation at the center of figure 3(b) represents the projected images of the parallel beam and of the drop located in the middle of the beam. The instant contact diameter of the drop, a key parameter of drop spreading, can be measured directly from the top-view photograph shown in figure 3(a), or from its projected image that represented by the dark circle at the center of figure 3(b). However, the latter has a large error in reading because its small image was embedded in a much larger shadowgraphic image and, therefore, cannot accurately be measured. One of the advantages of the method described in this article is the ability to record the top view of the drop and its reflection-refracted shadowgraphic image synchronously. The internal convective flow field of the drop can be visualized while the contact diameter and contact angle is accurately measured, and, therefore, effects of the flow motion on the spreading can be determined. For nonvolatile liquids, the sessile drop spreads calmly without any detectable internal flow convection, as shown in figure 3(b).

However, in volatile drops, evaporation can induce thermocapillary convection under certain conditions, depending on the properties of the liquid. Figures 4(a) to (c) depict the reflection-refracted shadowgraphic images of freon-113, n-pentane, and ethanol drops, respectively, evaporated on an aluminized glass plate in open air. The different evaporation rates and physical properties of the liquids produced different internal flow patterns and stabilities of the contact line. The thermocapillary convection in the freon-113 drops can be induced by evaporation from the very beginning, even before the syringe detaches from the drops. An instant reflection-refracted shadowgraph of a

freon-113 drop, shown in figure 4(a), clearly presents the typical four-region flow structure described by Zhang and Yang (refs. 1). The flow motion in the midway ring-shaped region of the drop is very strong, while a weak flow occurs in a very narrow region at the bottom of the drop, and a small stagnation region exists at the summit of the drop. On the other hand, the convection in n-pentane drops occurs after the drops spread for a short time. Before that, there is no convection in the drop at all. The flow pattern in the n-pentane drops is obviously different from that in the freon-113 drops. Active flow occurs at the bottom of the drop instead of in the midway ring-shaped region, where a weaker flow convection can be observed, leaving the top region stagnant.

The ethanol drops exhibit no flow motion throughout their lifetime as their evaporation rate is too low to induce thermocapillary convection. However, the ethanol drops develop an unstable three-phase contact line, where the interface tensions, contact angle, and Laplace capillary-pressure determine the shape of the interfaces. The unstable three-phase line gives a jagged periphery in the shadowgraphic image, as shown in figure 4(c). The instability of the three-phase line is attributed to the very high dielectric constant of ethanol and repulsive pressure at the drop edge (ref. 5).

To convincingly prove that the reflection-refracted shadowgraphic image qualitatively depicts the internal flow convection in a sessile drop, a freon-113 drop seeded with an aluminum-powder tracer was tested with the hybrid optical system. Figure 5 shows an instant top-view photograph of the drop and its corresponding reflection-refracted shadowgraph. Obviously, the tracer deformed the shape of the drop, causing different contact angles along the periphery, though the contact diameter still appears as a circle. However, the flow pattern depicted by the tracer in the direct photograph of the top view, shown in figure 5(a), is qualitatively similar to the shadowgraph shown in figure 5(b).

The reflection-refracted shadowgraphic image can also give comprehensive information of contact angle through the measurements of the diameter of the outmost fringe, D, and of the contact diameter of the drop from the top view, d. A method was developed to determine the contact-angle time-history from the shadowgraph. The shadowgraphic image collected on the screen at a predetermined distance from the substrate surface, $s = AB+BC$, where A denotes the drop center on the test plate, and B and C are its images on the reflector of Beam splitter III and the screen, as shown in figure 1. The rays are refracted out of the drop at an angle θ_r with the horizon and form the shadowgraphic image with a diameter D. By a simple geometric relationship, the following equation can be obtained:

$$\tan\theta_r = \frac{s}{(D+d)/2} \tag{1}$$

Both D and d are time dependent because of the spreading and evaporation, and can be accurately measured from the shadowgraphs and the top-view photographs, respectively. To determine the contact angle, θ, consider the detailed optical path near the drop edge shown in figure 2. Obviously, the angle θ_r equals $\left(\frac{\pi}{2} - \theta_2 + \theta\right)$, where θ_2 is the outgoing angle of the ray on the drop surface. Then, equation (1) can be rewritten as

$$\frac{2s}{D+d} = \frac{\cot\theta_2 + \tan\theta}{1 - \cot\theta_2 \tan\theta} \tag{2}$$

Applying Snill's law to each of the air-liquid interfaces and the reflection law to the substrate surface, θ_2 can be related to θ through the relation

$$\sin\theta_2 = n\sin 2\theta\sqrt{1 - \sin^2\theta/n^2} - \cos 2\theta\sin\theta \tag{3}$$

where n is the refractive index of the liquid. The contact angle, θ, can be obtained by solving the simultaneous equations (2) and (3).

Based on the sphere-cap approximation, the apex height of the drop h and the drop volume Ω can be expressed as

$$h = \frac{d(1-\cos\theta)}{2\sin\theta} \tag{4}$$

$$\Omega = \pi h^2 \left(\frac{d}{2\sin\theta} - \frac{h}{3} \right) \tag{5}$$

The average evaporation rate of the drop, W_{av}, is considered an important parameter to measure the evaporation strength and can be determined by

$$W_{av} = \frac{\Omega_0}{t_f} \tag{6}$$

where Ω_o is the initial volume of the tested sessile drop and t_f is the lifetime of the drop. The instant evaporation rate of a sessile drop, W, can be calculated by $W=\Delta\Omega/\Delta t$ where $\Delta\Omega\ (t)$ is the difference of volumes between the measuring time interval Δt.

Typical results of drop spreading, the contact-angle time-history, and the volume-time history are presented in figures 6 to 8. Figure 6 proves that for silicone oil (50 cSt.) drops, the drop spreading follows $d = k(t+a)^{1/7}$, Dodge's relation (ref. 8), that depicts the spreading law of a nonvolatile drop, and that the drop volume is unchanged. However, the spreading characteristics of volatile drops are quite different from that of nonvolatile drops. Generally, after a short initial spreading period, the drops approximately maintain a constant contact-diameter for a brief period, the so-called spreading-evaporation balance stage, followed by a monotonic contraction, referred to as the evaporation-dominant contraction stage. The spreading of an n-pentane drop, a cyclohexane drop, and many others exhibited the same characteristics. As shown in figure 7, the spreading of the n-pentane drop deviates from the Dodge relation (dish line) after the short initial spreading period and further in time, especially after the thermocapillary convection occurs when the spreading-evaporation balance stage ends. Although the evaporation rate of a freon-113 sessile drop, W_{av} = 0.126 μl/sec, is lower than that of an n-pentane sessile drop (W_{av} = 0.229 μl/sec), the initial spreading stage of a freon-113 drop is much shorter than that of an n-pentane drop. Additionally, no spreading-evaporation balance-stage is observed, as shown in figure 8. The spreading of the freon-113 drop deviates from Dodge's relation as depicted by the dish line from the very beginning because thermocapillary convection induced by evaporation has occurred. Evolutions of contact angle and volume for an n-pentane drop with an initial volume of 1.65 μl and for a freon-113 drop with an initial volume of 2.41 μl are plotted in figures 7 and 8, respectively.

Because the flow visualization was conducted simultaneously with the measurements of the spreading and dynamic contact angle, the effects of thermocapillary convection in a volatile drop on the spreading process are clearly shown.

CONCLUSIONS

The hybrid optical system consisting of reflection-refracted shadowgraphy and top-view photography is a unique technique for the measurements of spreading, instantaneous dynamic contact-angle, and volume time-history of a volatile drop on a nontransparent substrate. The merits of this technique are:

1. Because of nontransparency of the substrate and the spherical cap shape of the sessile drop, reflection-refracted shadowgraphy can be utilized for the visualization study of internal flow in volatile drops. The technique is not suitable for the study of volatile-liquid pools that have a flat interface.
2. The instantaneous drop size, including the contact diameter, contact angle, and drop volume can be accurately determined through the top-view photograph of the drop and its corresponding shadowgraphic image, which are synchronously recorded.
3. The comprehensive information of an evaporating drop on a nontransparent substrate, including the local contact angle along the periphery of the drop, the instability of the three-phase contact line, and the deformation of the drop shape, can be obtained and analyzed.
4. The effects of thermocapillary convective flow, induced by evaporation, on the spreading of volatile drops can be accurately investigated.

REFERENCES

1. N. Zhang and W.J. Yang, Microstructure of Flow inside Minute Drops Evaporating on a Surface, *ASME Journal of Heat Transfer*, Vol. 105, pp. 908–910, 1983.
2. N. Zhang and W.J. Yang, Visualization of Evaporative Convection in Minute Drops by Laser Shadowgraphy, *Rev. Sci. Instrum.*, Vol. 54, pp. 93–96, 1983.
3. W. Merzkirch, *Flow Visualization*, Academic Press, New York, 1974.
4. D.F. Chao and N. Zhang, Effects of Evaporation and Thermocapillary Convection on Spreading and Contact Angle of Volatile Droplets, *J. of Thermophysics and Heat Transfer*, (in print), 2001.
5. N. Zhang and W.J. Yang, Natural Convection in Evaporating Minute Drops, *ASME Journal of Heat Transfer*, Vol. 104, pp. 656–662, 1982.
6. N. Zhang and D.F. Chao, Effects of Evaporation/Condensation on Spreading and Contact Angle of a Volatile Drop, *Heat Transfer Science and Technology 2000*, (edited by B.-X. Wang), higher Education Press, Beijing, pp. 367–372, 2000.
7. C. Allain, D. Ausserre and F. Rondelez, A New Method for Contact-angle Measurements of Sessile Drops, *J. Colloid Interface Sci.*, Vol. 107, pp. 5–13, 1985.
8. F.T. Dodge, The Spreading of Liquid Droplets on Solid Surfaces, *J. Colloid Interface Sci.*, Vol. 121, pp. 154–160, 1988.

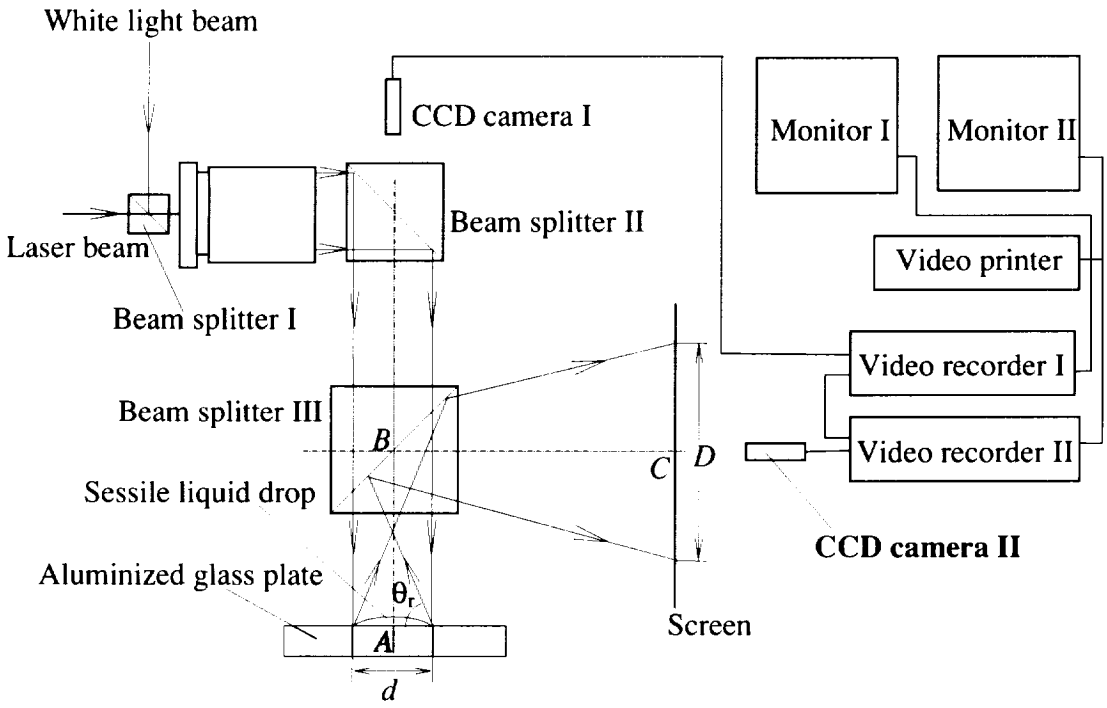

Figure 1.—Schematic of a hybrid optical system consisting of laser reflection-refracted shadowgraphy and direct photography.

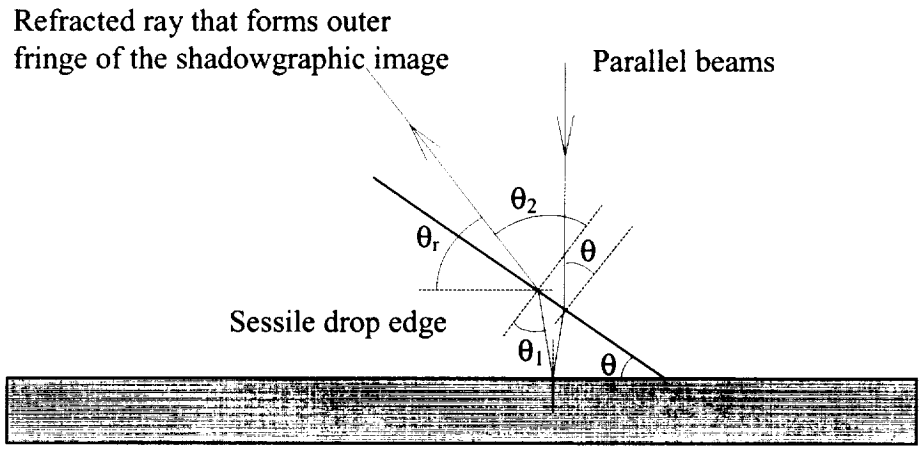

Figure 2.—Optical path at sessile drop edge.

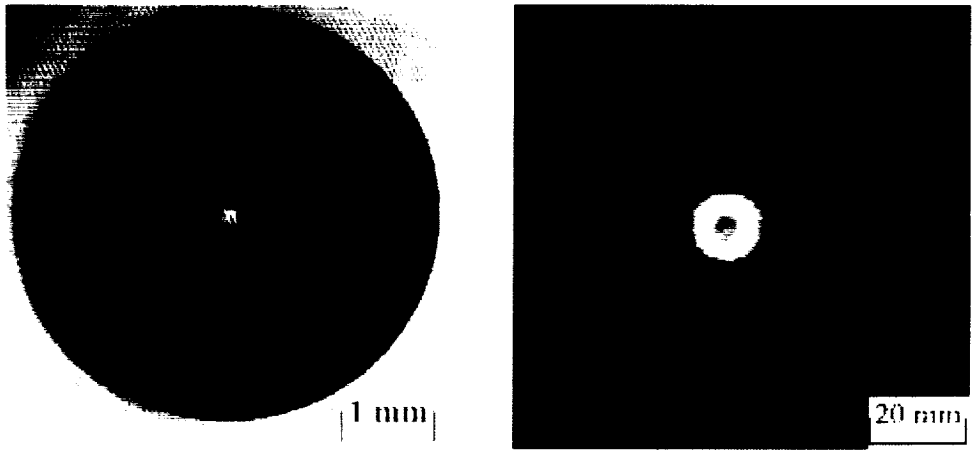

(a) top-view photograph (b) reflection-refracted shadowgraph

Figure 3.—Typical instant top-view photograph of a silicone-oil (50 cSt.) sessile drop and its corresponding reflection-reflected shadowgraph.

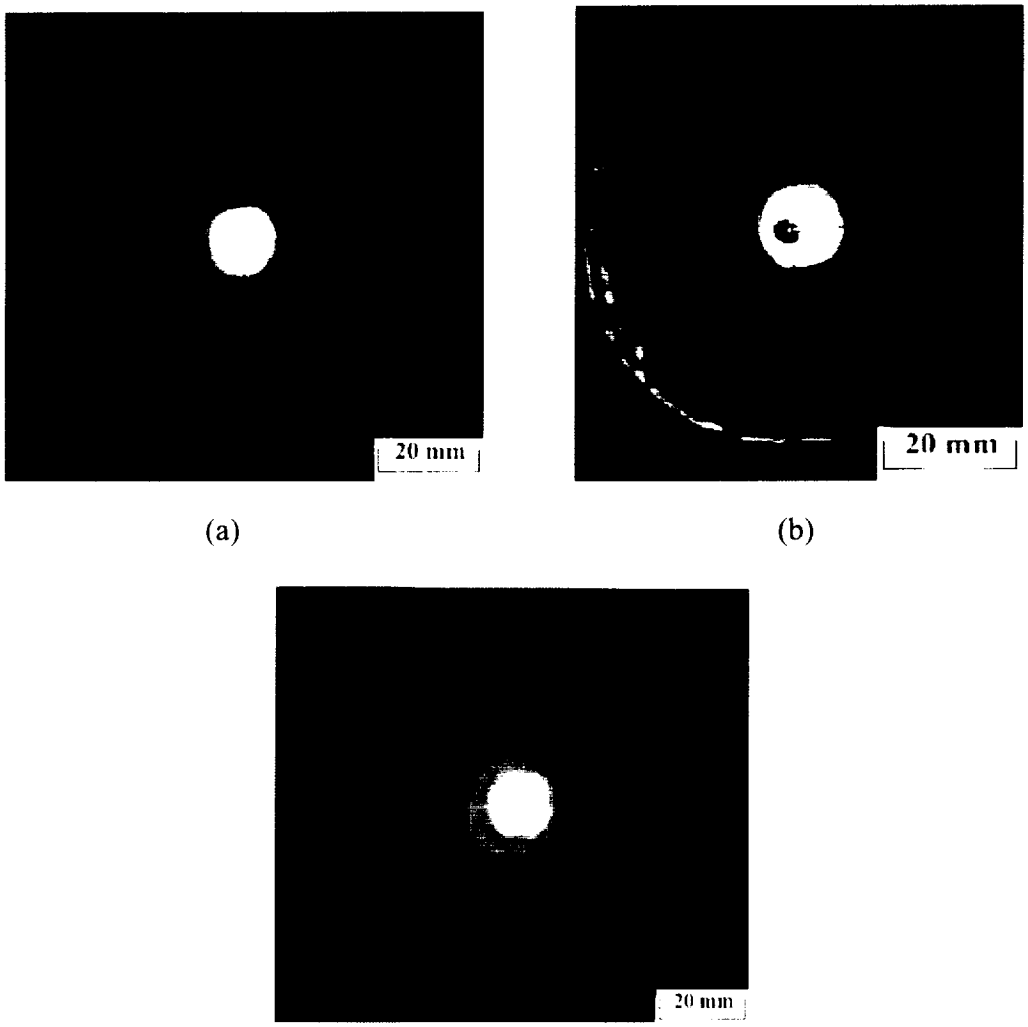

(a) (b)

(c)

Figure 4.—Instant reflection-refracted shadowgraphs of (a) freon-113, (b) n-pentane, and (c) ethanol drops evaporating on an aluminized glass plate in open air.

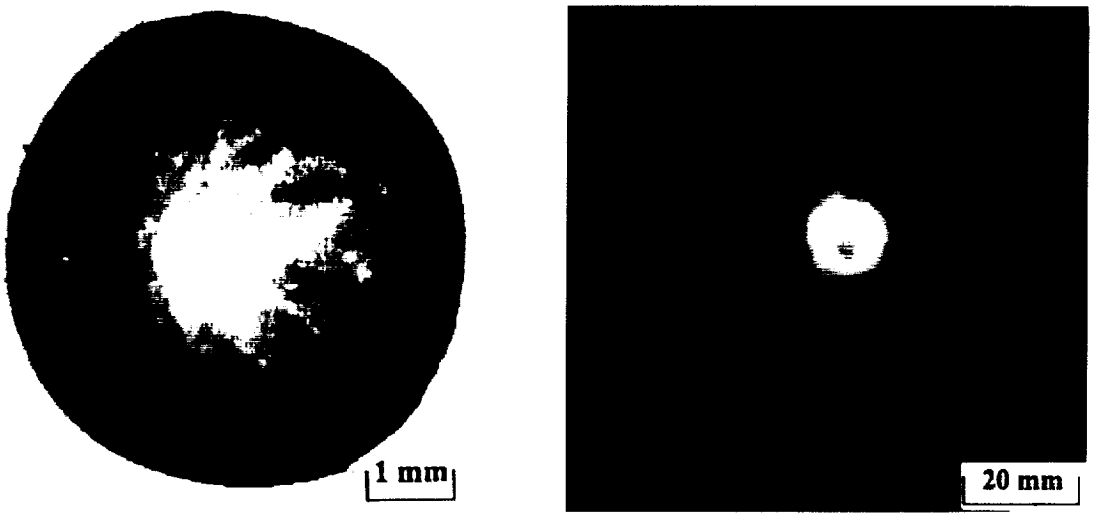

(a) top-view photograph (b) reflection-refracted shadowgraph

Figure 5.—Instant top-view photograph of a freon-113 drop with aluminum-powder tracer and its corresponding reflection-refracted shadowgraph.

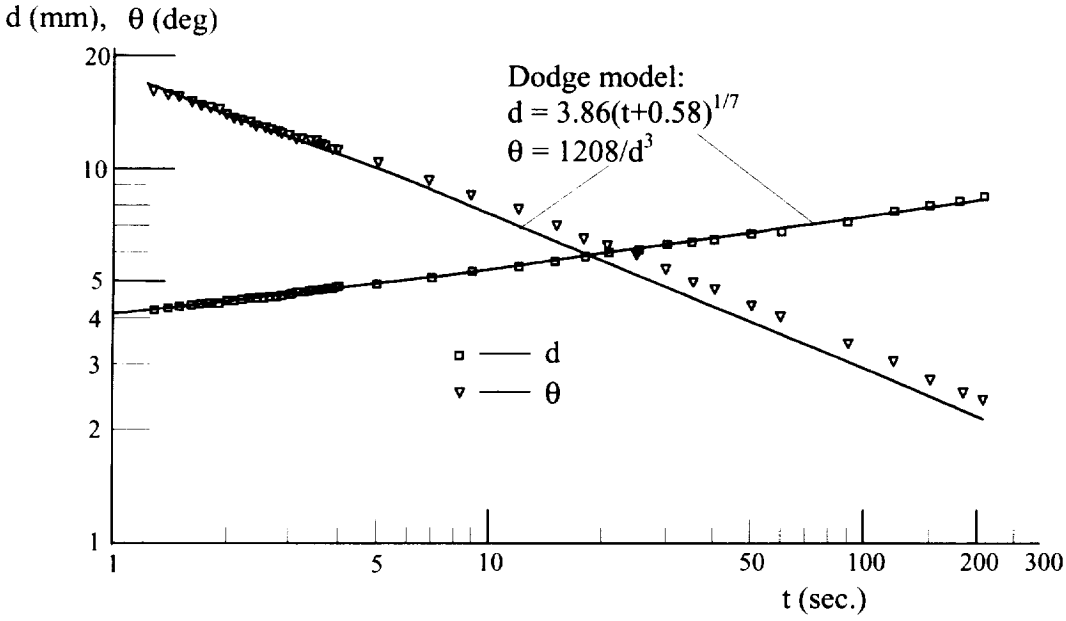

Figure 6.—Evolution of drop contact diameter, and contact angle for a silicone oil (50 cSt.) drop of volume 2.2 μl.

REPORT DOCUMENTATION PAGE

Form Approved
OMB No. 0704-0188

1. AGENCY USE ONLY (*Leave blank*)	2. REPORT DATE	3. REPORT TYPE AND DATES COVERED
	November 2001	Technical Memorandum

4. TITLE AND SUBTITLE

Flow Visualization in Evaporating Liquid Drops and Measurement of Dynamic Contact Angles and Spreading Rate

5. FUNDING NUMBERS

WU-101-53-00-00

6. AUTHOR(S)

Nengli Zhang and David F. Chao

7. PERFORMING ORGANIZATION NAME(S) AND ADDRESS(ES)

National Aeronautics and Space Administration
John H. Glenn Research Center at Lewis Field
Cleveland, Ohio 44135-3191

8. PERFORMING ORGANIZATION REPORT NUMBER

E-13084

9. SPONSORING/MONITORING AGENCY NAME(S) AND ADDRESS(ES)

National Aeronautics and Space Administration
Washington, DC 20546-0001

10. SPONSORING/MONITORING AGENCY REPORT NUMBER

NASA TM—2001-211284

11. SUPPLEMENTARY NOTES

Prepared for the 2001 International Mechanical Engineering Congress and Exposition sponsored by the American Society of Mechanical Engineers, New York City, New York, November 11–16, 2001. Nengli Zhang, Ohio Aerospace Institute, 22800 Cedar Point Road, Brook Park, Ohio 44142, and David F. Chao, NASA Glenn Research Center. Responsible person, David F. Chao, organization code 6712, 216–433–8320.

12a. DISTRIBUTION/AVAILABILITY STATEMENT

Unclassified - Unlimited
Subject Category: 34 Distribution: Nonstandard

Available electronically at http://gltrs.grc.nasa.gov/GLTRS
This publication is available from the NASA Center for AeroSpace Information, 301–621–0390.

12b. DISTRIBUTION CODE

13. ABSTRACT ***(Maximum 200 words)***

A new hybrid optical system, consisting of reflection-refracted shadowgraphy and top-view photography, is used to visualize flow phenomena and simultaneously measure the spreading and instant dynamic contact angle in a volatile-liquid drop on a nontransparent substrate. Themocapillary convection in the drop, induced by evaporation, and the drop real-time profile data are synchronously recorded by video recording systems. Experimental results obtained from this unique technique clearly reveal that thermocapillary convection strongly affects the spreading process and the characteristics of dynamic contact angle of the drop. Comprehensive information of a sessile drop, including the local contact angle along the periphery, the instability of the three-phase contact line, and the deformation of the drop shape is obtained and analyzed.

14. SUBJECT TERMS

Thermocapillary convection; Dynamic contact angles; Spreading; Nontransparent substrate

15. NUMBER OF PAGES

15

16. PRICE CODE

17. SECURITY CLASSIFICATION OF REPORT	18. SECURITY CLASSIFICATION OF THIS PAGE	19. SECURITY CLASSIFICATION OF ABSTRACT	20. LIMITATION OF ABSTRACT
Unclassified	Unclassified	Unclassified	

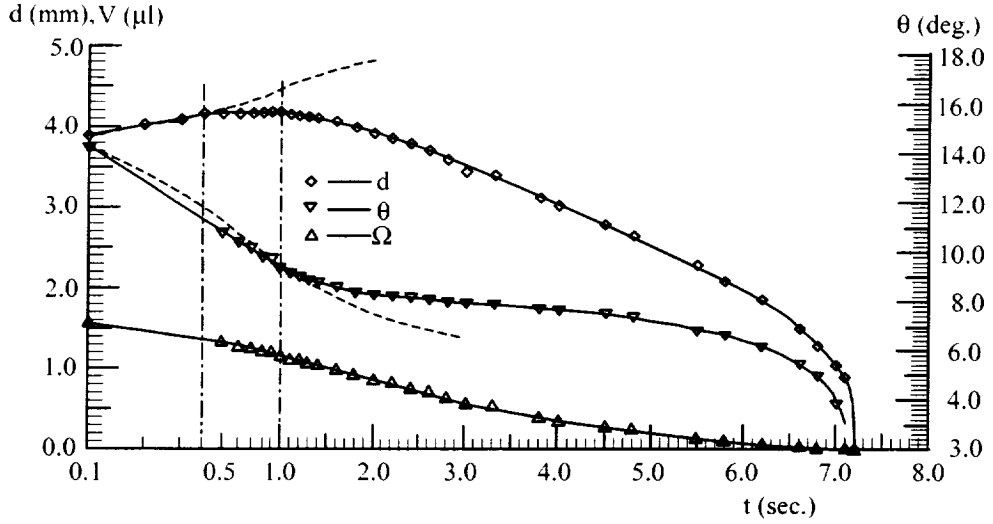

Figure 7.—Evolution of drop contact diameter, contact angle, and volume for an n-pentane drop of initial volume 1.65 μl.

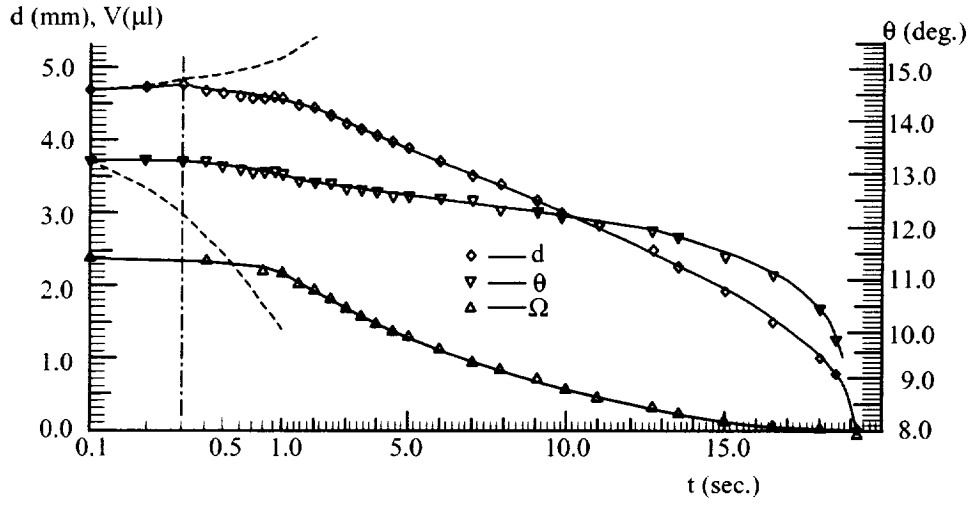

Figure 8.—Evolution of drop contact diameter, contact angle, and volume for a freon-113 drop of initial volume 2.41 μl.